

NILU  
TEKNISK NOTAT NR 1 /80  
REFERENCE: 22279  
DATE: JANUARY 1980

ON THE PREDICTION OF HAZARD AREA  
RESULTING FROM A GAS RELEASE

BY

K.J. EIDSVIK

NORWEGIAN INSTITUTE FOR AIR RESEARCH  
P.O. BOX 130, 2001 LILLESTRØM  
NORWAY

ISBN-82--7247-157-4

CONTENT

	Page
SUMMARY .....	5
1 INTRODUCTION .....	7
2 THE MODEL .....	8
2.1 Concentration distribution .....	8
2.1.1 Relative concentration distribution .....	9
2.1.2 Centre of gravity distribution .....	10
2.2 Actual and predicted hazard .....	13
2.2.1 Transverse dimension .....	13
2.2.2 Longitudinal dimension .....	15
2.3 Predicted hazard area .....	17
3 CHARACTERISTIC VALUES .....	19
3.1 Maximum hazard time .....	19
3.2 Maximum hazard distance .....	20
3.3 Transverse dimension .....	21
4 CONCLUDING REMARKS .....	22
5 REFERENCES .....	24



SUMMARY

The size of the predicted hazard area following the release of a hazardous gas cloud is estimated to depend more upon prediction error for actual atmospheric flow and flow parameters than upon the accuracy of the diffusion model for given flow parameters. At a fixed risk level, the size of the predicted hazard area could be halved by using accurate prediction methods for the actual atmospheric flow (parameters).



## ON THE PREDICTION OF HAZARD AREA RESULTING FROM A GAS RELEASE

### 1 INTRODUCTION

If explosive or poisonous gases have been released to the atmosphere, it may be necessary to estimate the areas and times where the risks are unacceptable. If activities to minimize damage are required, these should be directed towards areas where they probably can give results, and not towards areas where they probably would be wasted. Unconditional "worst case" prediction results in a much larger predicted hazard area than is necessary. We should not be satisfied with this if the undesirable effects can be minimized more effectively by utilizing the weather variations in the predicted hazard area. The objective is, therefore, to obtain as small a predicted hazard area as is "cost-effective" at a given risk level.

For simplicity it is assumed that the hazard is associated with an instantaneous gas concentration,  $\chi$ , above a hazard limit  $\chi_h$ , and that the cloud is generated instantaneously. When dealing with instantaneous concentrations, the differences between the relative spread in a puff and in an element of a continuous plume are small. A plume may then be considered to be composed of a series of puffs. To be specific, the scale is associated with a maximum hazard time and along-wind distances of the order  $T_h = O(10 \text{ min})$  and  $\theta_1 = O(1 \text{ km})$ , respectively.

The traditional efforts to predict gas cloud behaviour in the atmosphere have mostly been directed towards accurate prediction of mean cloud size given the actual flow parameters. Exceptions like Gifford's fluctuating plume model (1) and other models have been summarized by Csanady (2). The present report is an exploratory effort to make different meteorological aspects of the prediction of hazard area sufficiently explicit so as to allow estimation of what aspects are the more important ones. The

(practical) importance is a main reason for working with gas cloud behaviour at all.

Rough ideas on how to proceed are obtained from the following findings: i) the spectrum of atmospheric wind has most energy at the larger scales of motion (Lumely and Panofsky, 3); ii) the atmospheric eddies that contribute most to the dispersion of a cloud are of the same dimensions as the cloud (Pasquill, 4); iii) the atmospheric eddies that contribute most to the cloud's centre of gravity motion are of larger dimensions than the cloud; iv) cloud behaviour varies considerably with the flow parameters (4). The first three statements indicate that the size of the predicted hazard area depends more upon the prediction error for the centre of gravity location than on cloud dispersion. The last statement suggests that the size of the predicted hazard area depends much on the estimation errors for actual flow parameters. These ideas, illustrated in Figure 1, will now be discussed in a more explicit form.

## 2 THE MODEL

### 2.1 Concentration distribution at fixed locations

The probability of hazard depends on the stochastic concentration field,  $\chi(\underline{x}, t)$ , in space and time. A complete statistical description of this non-stationary and non-homogeneous field is beyond reach. It is estimated that the largest fluctuations are associated with the largest eddies, of the same size as the cloud itself (Eidsvik, 5). Inside the mean cloud the probability of simultaneous high concentrations is therefore high. A relevant, nontrivial aspect is therefore the probability density function of concentration at fixed spatial and time coordinates  $\beta(\chi; \underline{x}, t)$ . This distribution is considered conditional to the atmospheric flow.

It is convenient to discuss the spreading of a puff in terms of



the centre of gravity motion and the relative dispersion. When the source strength is  $Q$  and the Lagrangian centre of gravity velocity  $\underline{u}(t)$ , the centre of gravity vector,  $\underline{c}(t)$ , is:

$$\begin{aligned} \underline{c}(t) &= Q^{-1} \int \underline{x} \chi(\underline{x}, t) d\underline{x} \\ &= \int_0^t \underline{u}(\underline{c}(\tau)) d\tau, \end{aligned} \quad (2.1)$$

The probability density for the stochastic  $\underline{c}$ -vector is  $\beta(\underline{c}, t)$ . A non-trivial statistical property of relative diffusion is the probability density for concentration at fixed spatial and time coordinates, given the centre of gravity vector  $\beta(\chi; \underline{r}, t) = \beta(\chi/\underline{c}; \underline{x}, t)$  ~~with~~  $\underline{r} = \underline{x} - \underline{c}$ . The joint density of the two stochastic variables, concentration and centre of gravity vector, is then  $\beta(\chi, \underline{c}; \underline{x}, t) = \int \beta(\chi; \underline{r}, t) \beta(\underline{c}; t) d\underline{c}$ , so that the marginal probability density of interest is formally given as:

$$\beta(\chi; \underline{x}, t) = \int \beta(\chi; \underline{r}, t) \beta(\underline{c}; t) d\underline{c}, \quad (2.2)$$

or, in terms of distribution functions:

$$F(\chi; \underline{x}, t) = \int F(\chi; \underline{r}, t) \beta(\underline{c}; t) d\underline{c} \quad (2.3)$$

### 2.1.1 Relative concentration distribution

Experimental evidence indicates that the relative concentration distribution may be approximated as:

$$F(\chi; \underline{r}, t) = \begin{cases} F(0) & , \text{ for } \chi = 0, \\ \frac{1}{2} [1 + \operatorname{erf}(\frac{\ln \chi / \chi_0}{\sqrt{2} \sigma_*})] & , \text{ if } \chi > 0, \end{cases} \quad (2.4)$$

with parameters  $F(0; \underline{r}, t)$ ,  $\chi_0(\underline{r}, t)$ ,  $\sigma_*(\underline{r}, t)$ , and

$$\operatorname{erf}(\lambda) = \frac{2}{\sqrt{\pi}} \int_0^\lambda e^{-t^2} dt = 2 \int_0^{\sqrt{\pi} \lambda} n(0, 1) d\tau \quad (2.5)$$

Most literature on the subject of turbulent diffusion is concerned with properties of the first moment,  $\bar{\chi}(\underline{r}, t)$ . For a passive scalar cloud this moment is commonly found to have spatially Gaussian profiles. With proper orientation of coordinate axes, the  $\bar{\chi}$ -field may then be discussed in terms of standard deviations,  $\sigma_i(t)$ ;  $i = 1, 2, 3$ . A "heavy gas" cloud is expected to have a more uniform spatial profile of mean concentration (Eidsvik, 6). However,  $\sigma_i$  is in any case understood to be a measure of the mean cloud dimension.

Smith and Hay's (7) estimate for the isotropic  $\sigma_i(t)$  illustrates the transfer function between the turbulence and the growth of a cloud:

$$\frac{d\sigma_i}{dt} \approx \frac{3}{U} \int_0^{\infty} E(k) \kappa(k) dk \quad , \quad (2.6)$$

$$\kappa(k) = (\sigma_i k)^{-1} [1 - e^{-(\sigma_i k)^2}] \quad , \quad (2.7)$$

Here  $U$  is the mean wind, and  $E(k)$  is the Eulerian three-dimensional wave number turbulence spectrum. The transfer function,  $\kappa(k)$ , shows that the most efficient atmospheric eddies are of the same dimensions as the cloud.

### 2.1.2 Centre of gravity distribution

In an actual case of gas release, the centre of gravity vector must be predicted as:

$$\begin{aligned} \hat{\underline{c}}(t) &= \int_0^t \hat{\underline{u}}(\hat{\underline{c}}(\tau)) d\tau \quad , \\ &\approx \hat{\underline{u}} t \quad , \end{aligned} \quad (2.8)$$

where  $\hat{\underline{u}}$  is the predicted atmospheric wind along the predicted trajectory. The prediction error is:

$$\begin{aligned}
 \underline{c}'(t) &= \underline{c}(t) - \hat{\underline{c}}(t) \\
 &= \int_0^t [\underline{u}(\underline{c}(\tau)) - \hat{\underline{u}}(\hat{\underline{c}}(\tau))] d\tau \quad (2.9) \\
 &\approx \int_0^t [\underline{u}(\hat{\underline{c}}(\tau)) - \hat{\underline{u}}(\hat{\underline{c}}(\tau))] d\tau .
 \end{aligned}$$

As indicated by Eidsvik (8), it may be difficult to estimate  $\underline{u}$  significantly more accurate than to be constant over horizontal coordinates and time. Since the extrapolation distances in space and time associated with this prediction are normally much larger than the difference between  $\underline{c}$  and  $\hat{\underline{c}}$ , the transcendental and Lagrangian character of Equation (2.9) is avoided by replacing  $\underline{c}$  with  $\hat{\underline{c}}$  on the right hand side.

It is convenient to consider  $\underline{x}$  and  $\underline{c}$  to be vectors in a coordinate system moving with  $\hat{\underline{c}}$ , and orient the system so that the  $x_1$ -axis is along the predicted, but not necessarily constant, wind. The distribution of the prediction error for the centre of gravity location is then  $\beta(\underline{c};t)$ . With this interpretation of  $c = \underline{c}'$ , Giffords (1) and Csanady's (2) results on puff diffusion are applicable to the present problem. However,  $\beta(\underline{c};t)$  can now be controlled. For accurate prediction methods,  $\beta(\underline{c};t)$  is assumed to be nearly Gaussian. Unbiased prediction methods may then be characterized with the prediction variance,  $Ec_i^2(t)$ , given as a functional of atmospheric wind by Equation (2.9).

The filtering of atmospheric fluctuations by Equation (2.9) is illustrated with the following simple model: the clouds trajectory is assigned to the coordinate of its predicted center of gravity over the diffusion interval,  $(\underline{x}_0, t_0)$ . The last and nearest measurement occurs without error at  $(\underline{x}_1, t_1)$ . When predicting with the measured value and the integral scale for the eddies to be predicted is large, Equation (2.9) becomes approximately:

$$[\underline{c}(\underline{x}_0, t_0) - \underline{c}(\underline{x}_1, t_1)] \approx t[\underline{u}(\underline{x}_0, t_0) - \underline{u}(\underline{x}_1, t_1)]. \quad (2.10)$$

The variance in the  $\hat{c}$  system is then:

$$\begin{aligned} E\{c_i^2\} &\approx t^2 E[u_i(\underline{x}_0, t_0) - u_i(\underline{x}_1, t_1)]^2 \\ &\approx t^2 D_{ii}(\underline{x}_0 - \underline{x}_1, t_0 - t_1). \end{aligned} \quad (2.11)$$

Assuming  $\|(\underline{x}_0, t_0) - (\underline{x}_1, t_1)\| \gg t$ , and Taylor's hypothesis to be valid, this may be written:

$$E\{c_i^2\} \approx t^2 D_{ii}(\underline{y}), \quad (2.12)$$

with

$$\underline{y} = \underline{x}_0 - \underline{x}_1 + \underline{U}(t_0 - t_1). \quad (2.13)$$

The spectral form of Equation (2.12) reads

$$\begin{aligned} E\{c_i^2\} &= 2t^2 \int_{\underline{k}} \phi_{ii}(\underline{k}) [1 - e^{-i\underline{k} \cdot \underline{y}}] d\underline{k} \\ &= 8t^2 \int_0^\infty \phi_{ii}(k_y) \sin^2 \frac{k_y \cdot y}{2} dk_y \end{aligned} \quad (2.14)$$

Here  $\phi_{ii}(k_y)$  is the one-dimensional velocity spectrum along the direction of  $y$ . The filter,  $\sin^2 \frac{k_y y}{2}$ , shows that the contribution from atmospheric eddies of dimensions larger than approximately  $\{\underline{x}_0 - \underline{x}_1, t_0 - t_1\}$  is damped. However, as  $\phi_{ii}(k_y)$  has most energy at low wave-numbers, the atmospheric eddies that contribute most are of approximately the same dimensions as the distance (in time and space) between the last measurement and the center of gravity for the clouds trajectory (compare Eidsvik, 9).

## 2.2 Actual and predicted hazard

The actual hazard occurs in the stochastic area around  $\underline{c}(t)$  where  $\chi > \chi_h$ . With some account taken for vertical integration of actual concentration, the ground level hazard area at time  $t$  may be expressed as an integral of the Heavyside function,  $H(\chi(r_1, r_2, 0, t) - \chi_h)$ , as :

$$\int H(\chi(r_1, r_2, 0, t) - \chi_h) dr_1 dr_2. \quad (2.15)$$

The hazard must be predicted in the area where the distribution  $F(\chi_h; \underline{x}, t)$  (or  $F(\chi_h; \underline{x}, t)$  at some time) exceeds an unacceptable value. The risk,  $P_h$ , may vary several orders of magnitudes with the particular occasion and/or purpose. However, as the distributions used are only approximations for commonly occurring concentrations,  $P_h$  should be restricted to  $P_h \geq 0(10^{-2})$ .

Since the predicted hazard area must be geometrically simple, it is sufficient to discuss simple aspects of the actual and predicted hazard area only. The attention is, for instance, directed towards two convenient time intervals: times in the neighbourhood of vanishing hazard,  $T_h$ , and intermediate times,  $0 \ll t \ll T_h$ .

### 2.2.1 Transverse dimension

For  $t \ll T_h$  and  $\chi_0(\underline{r}=0) \gg \chi_h$ , the probability of simultaneous hazards at two locations closer together than the size of the cloud will be high, so that most of the actual hazard area will be confined to a compact region around the location of the actual gravity centre. Since  $\chi_0(\underline{r}=0) \gg \chi_h$ , there will be small differences between the areas bounded by  $\chi > \chi_h$  and  $\chi > 0$ . The most important aspect of hazard area characteristic appears to be the area size. To be specific, the actual hazard area may be represented as an ellipse with "optimal" shape and orientation, or more simply, a circle of radius,  $s$ , with the same area as the actual hazard area.

$$s^2(t) = \frac{1}{\pi} \int H(\chi(r_1, r_2, 0, t) - \chi_h) dr_1 dr_2$$

$$\approx \frac{1}{\pi} \int H(\chi(r_1, r_2, 0, t)) dr_1 dr_2. \quad (2.16)$$

The predicted, instantaneous hazard area could be defined as the circle with radius  $\theta_2(t)$  around the predicted location of the centre of gravity, such that the probability of hazard outside this circle is smaller than  $P_h$ :

$$P\{S(t) + c(t) > \theta_2(t)\} = P_h. \quad (2.17)$$

When the interest is only on the transverse dimension of the predicted hazard area, as is assumed there,  $c(t)$  is replaced by the transverse component  $c_2(t)$ . The distributions of  $s(t)$  and  $c_2(t)$  are in principle given by Equation (2.16) and  $\beta(\underline{c}; t)$ . Already the first moment of  $s$  would require knowledge of the intermittency factor,  $F(0; \underline{r}, t)$ . Since  $H(\chi(\underline{r}, t)) = 0$  with probability  $F(0; \underline{r}, t)$ , and  $H(\chi(\underline{r}, t)) = 1$  with probability  $1 - F(0; \underline{r}, t)$ ,  $E\{H(\chi(\underline{r}, t))\} = 1 - F(0; \underline{r}, t)$ , so that Equation (2.16) gives:

$$Es^2(t) = \frac{1}{\pi} \int [1 - F(0; \underline{r}, t)] dr_1 dr_2. \quad (2.18)$$

The large uncertainty associated with the stochastic structure of  $s(t)$  implies that simple estimates should be used. The dominance of the large scale eddies in the atmosphere, implying a large  $c_2$  compared to  $s$ , is another argument for using simple estimates for the distribution of  $s$ . We suggest that  $\beta(s)$  is nearly  $n(\mu_s, \sigma_s)$ . Then  $(s + c_2)$  is  $n(\mu_s; \sigma)$  with  $\sigma^2 = \sigma_s^2 + Ec_2^2 \approx Ec_2^2$ , so that  $\theta_2$  is obtained from Equation (2.17) as:

$$\frac{\theta_2^2 - \mu_s}{\sigma_s} = \frac{1}{2} (1 - P_h)$$

$$\operatorname{erf}\left(\frac{\theta_2 - \mu_s}{\sqrt{2}\sigma}\right) = (1 - P_h)$$

$$\begin{aligned}\theta_2(t) &= \mu_s(t) + \sqrt{2}\sigma(t)\operatorname{erf}^{-1}(1 - P_h) \\ &= \mu_s(t) + \alpha_1\sigma(t)\end{aligned}\tag{2.19}$$

The first moment of  $s(t)$ ,  $\mu_s(t)$ , could be formally obtained from Equation (2.18). Again, due to the large uncertainty of  $F(0; \underline{r}, t)$  we rather restrict the time to intervals where  $\mu_s(t) \approx 0(2\sigma_1)$  so that:

$$\theta_2(t) \approx 2\sigma_1(t) + \alpha_1\{Ec_2^2(t)\}^{\frac{1}{2}}.\tag{2.20}$$

If hazards of the order of  $P_h \approx 0(10^{-1})$  are accepted,  $\alpha_1 \approx 2$ . If only extremely small hazards are acceptable,  $\alpha_1 \gg 2$ . For an initially small passive scalar cloud the large scale atmospheric fluctuations will contribute significantly to  $Ec_2^2(t)$  and not to  $\sigma_2^2(t)$ , so that the prediction error term in Equation (2.20) will normally dominate in any case.

### 2.2.2 Longitudinal dimension

In the neighbourhood of the maximum hazard time,  $T_h$ , or distance,  $\theta_1$ , the condition  $\chi > \chi_h$  occurs in the central portion of the mean cloud. The actual hazard area is now expected to be disconnected, so that the  $s(t)$  of Equation (2.16) may no longer be relevant for describing the actual hazard. However, the probability of simultaneous hazards at two locations closer together than  $\sigma_1$  is still relatively high (5). A reasonable predicted maximum hazard time,  $T_h$ , is then obtained by requiring the probability at the most hazardous location,  $\underline{r} = 0$ , to be small enough:

$$F(\chi = \chi_h; \underline{r} = 0, T_h) = P_h.\tag{2.21}$$

In the central portion of the cloud the intermittency factor is small so that the concentration distribution is approximately log-normal.

$$\frac{1}{2} [1 + \operatorname{erf}(\frac{\ln \chi_h / \chi_o}{\sqrt{2} \sigma_*})] = P_h,$$

$$\frac{\chi_h}{\chi_o} = \exp[\sqrt{2} \sigma_* \operatorname{erf}^{-1}(1 - 2P_h)]$$

$$= \exp(\alpha_2 \sigma_*).$$
(2.22)

In terms of the mean value,  $\bar{\chi}$ , this may be written:

$$\bar{\chi}(T_h) = \chi_h \exp[-\alpha_2 \sigma_* + \frac{1}{2} \sigma_*^2].$$
(2.23)

For  $P_h \leq 0(10^{-1})$  and  $\sigma_* \approx 0.5$  the first term of the exponential dominates. Inversion of the Equation (2.23) then gives:

$$T_h = \bar{\chi}^{-1} \{ \chi_h \exp[-\alpha_2 \sigma_* + \frac{1}{2} \sigma_*^2] \}$$

$$\approx \bar{\chi}^{-1} \{ \chi_h \exp[-\alpha_2 \sigma_*] \}.$$
(2.24)

The predicted maximum hazard distance,  $\theta_1$ , is determined by the location of  $c(T_h)$ , or  $c_1(T_h)$ , plus a small "correlation distance",  $O(\sigma_1(T_h))$ , for the concentration field. A specific definition is obtained by requiring the probability of a larger  $c_1$  value than  $c_*(T_h)$  to be  $P_h$ .

$$c_*(T_h) = \{ E c_1^2(T_h) \}^{\frac{1}{2}} \operatorname{erf}^{-1}(1 - 2P_h),$$

$$c_*(T_h) = \alpha_2 \{ E c_1^2(T_h) \}^{\frac{1}{2}}.$$
(2.25)



For risks of the order  $P_h = O(10^{-1})$  the coefficient  $\alpha_2$  is approximately 2. The predicted maximum distance, measured from the source becomes:

$$\begin{aligned} \theta_1 &\approx \int_0^{T_h} \hat{u}_1(\tau) d\tau + c_*(T_h) + \sigma_1(T_h) \\ &\approx \hat{u}_1 T_h + c_*(T_h) + \sigma_1(T_h) \end{aligned} \quad (2.26)$$

### 2.3 Predicted hazard area

A reasonably rational way to estimate the predicted hazard area with known flow structure has been developed. The predicted hazard area is characterized by  $T_h$  of Equation (2.24),  $\theta_1$  of Equation (2.26), and  $\theta_2$  of Equation (2.20). The quantile  $\underline{\theta} = \{\theta_1, \theta_2, T_h\}$  of the approximate order  $1 - P_h$ , depend upon the atmospheric diffusion parameter vector,  $\underline{\mu} = \{\sigma_1, \bar{\chi}, \sigma_*, Ec_1^2\}$ , through the equations developed. The diffusion parameters depend in turn on the atmospheric flow parameter vector,  $\underline{v}$ , so that the relations may formally be written:

$$\underline{\theta} = \underline{\theta}(\underline{\mu}(\underline{v})). \quad (2.27)$$

In an actual situation of gas release, the parameters must be estimated (predicted). The uncertainty associated with this is treated analogously to interval estimation of parameters: the available information is a prediction of atmospheric flow parameters,  $\hat{v}_k$ , with prediction error  $\Delta v_k$ . For hazard estimation an unfavourable parameter must be chosen, say  $\tilde{v}_k$  (conditionally worst case). For simplicity  $\hat{v}_k$  is assumed to be nearly normally distributed, so that the unfavourable  $\tilde{v}_k$  is chosen at the risk level  $P_h^* = O(P_h)$  as:

$$\begin{aligned} \tilde{v}_k &= \hat{v}_k \pm \sqrt{2} \Delta v_k \operatorname{erf}^{-1}(1 - P_h^*) \\ &= \hat{v}_k \pm \alpha_1^* \Delta v_k \end{aligned} \quad (2.28)$$

The minus sign is chosen when a small  $v_k$  is most hazardous. Except for  $\sigma_*$ , for which an accurate model is unknown, the dispersion models,  $\hat{\mu}(v)$ , have received so much attention that their errors are not discussed here. With given  $\Delta v_k$ , a small diffusion model error may not even result in a small prediction error for  $\mu_i$ . This may be so if the "real"  $\mu_i$  varies much over intervals of  $v_i$  that are smaller than  $\Delta v_i$ . Busch (10) has indicated that the atmosphere may actually have such a property in the neighbourhood of the commonly occurring "near neutral conditions". When the estimated relations for  $\underline{\theta}(v)$  are called  $\hat{\theta}$ :

$$\tilde{\theta} = \hat{\theta}(\hat{\mu}(\tilde{v})) = \hat{\theta}(\tilde{\mu}) \quad , \quad (2.29)$$

where  $\tilde{\mu}_i$  means  $\hat{\mu}_i(v)$  when models exist, and  $\tilde{\sigma}_* = \hat{\sigma}_* + \alpha_1^* \Delta \sigma$  for  $\mu_i = \sigma_*$ . Application of Equation (2.29) to the Equations (2.20), (2.24), (2.25) and (2.26) gives the predicted hazard area characteristics:

$$\tilde{\theta}_2(t) \approx 2 \tilde{\sigma}_2(t) + \alpha_1 [E(c_2^2(t))]^{1/2} \quad , \quad (2.30)$$

$$\tilde{T}_h \approx \tilde{\chi}^{-1} \{ \chi_h \exp[-\alpha_2 \tilde{\sigma}_*] \quad , \quad (2.31)$$

$$\tilde{\theta}_1 \approx \hat{u}_1 \tilde{T}_h + \tilde{c}_*(\tilde{T}_h) + \tilde{\sigma}_1(\tilde{T}_h) \quad . \quad (2.32)$$

For a given approximate risk,  $P_h$ , the control variables for the size of the predicted hazard area are  $Ec_1^2(t)$ ,  $\Delta \sigma_i$ ,  $\Delta \bar{\chi}$  and  $\Delta \sigma_*$ .

### 3 CHARACTERISTIC VALUES

#### 3.1 Maximum hazard time

The computation of  $\tilde{T}_h$  requires an equation for  $\bar{\chi}(t)$ . Using the simple estimate suggested by Smith and Hay (7) for an initially small cloud, gives:

$$\sigma_i(t) \approx \begin{cases} 3 \frac{\sigma_u^2}{U} t & \text{for } \sigma_1 < O(UL) \\ 2\sigma_u \sqrt{Lt} & \text{for } \sigma_1 \gg O(UL) \end{cases}, \quad i=1,2,3 \quad (3.1)$$

Here  $U$  is the mean wind,  $\sigma_u^2$  the variance and  $L$  the Lagrangian integral scale of the small scale wind fluctuations. With Equation (3.1) introduced into a Gaussian dispersion formula, the maximum concentration is given as a function of  $t$ . Substitution into Equation (2.31) then gives the predicted hazard time.

$$\tilde{T}_h \approx \begin{cases} \frac{1}{3\sqrt{2}\pi} \left[ \frac{\tilde{Q}}{\chi_h} \right]^{1/3} \exp\left(\frac{\alpha_2}{3} \tilde{\sigma}_*\right) \left[ \frac{\tilde{U}}{\tilde{\sigma}_u^2} \right], & \text{for } \sigma_1(T_h) \leq O(UL) \\ \frac{1}{8\pi} \left[ \frac{\tilde{Q}}{\chi_h} \right]^{2/3} \exp\left(\frac{2\alpha_2}{3} \tilde{\sigma}_*\right) \left[ \frac{1}{L\tilde{\sigma}_u^2} \right], & \text{for } \sigma_1(T_h) \gg UL \end{cases} \quad (3.2)$$

Logarithmic variation of the Equation (3.2) indicates that  $\tilde{T}_h$  varies less rapidly with prediction error for release mass, compared with prediction errors for the parameters  $\{\sigma_*, U, \sigma_u, L\}$ .

The increase in  $T_h$  due to concentration fluctuations and their uncertainty is given by the exponential term of Equation (3.2). The scarcity of data for  $\sigma_*$  justify the simple approximation of assuming  $\sigma_*$  to be approximately constant over the central portion of the cloud (2,5). For  $\hat{\sigma}_* \approx \Delta\sigma_* \approx 0.5$  and  $P_h \approx O(10^{-1})$  the "safety factor" for  $T_h$  due to concentration fluctuations becomes approximately 1.5.

The increase in  $T_h$  due to prediction errors for actual flow parameters,  $\{U, \sigma_u, L\}$ , is given by the last factor in Equation (3.2). The estimation errors for  $U$ ,  $\sigma_u$  and  $L$  are likely to be of the orders  $\Delta U = O(0.3U)$ ,  $\Delta\sigma_u = O(\sigma_u)$  and  $\Delta L = O(L)$ , respectively. These prediction errors may therefore increase the predicted hazard time from  $T_h$  to  $\tilde{T}_h$  by a factor of approximately 2. This type of error may also be illustrated with prediction error of actual "Pasquill stability class" (4).

An accurate prediction (estimation) method for actual weather parameters could reduce the predicted maximum hazard time by approximately 2. The predicted maximum hazard time may be approximately 3 times larger than the value obtained from the most accurate conventional diffusion model.

### 3.2 Maximum hazard distance

A lower limit for  $c_*(T_h)$  is obtained from Equation (2.12) as:

$$c_*(T_h) \geq \alpha_2 D_{11}^{\frac{1}{2}}(T_h) T_h \quad (3.3)$$

A representative estimate for the small scale turbulence over a water surface is (Eidsvik and Panofsky, 11):

$$\sigma_u \approx 10^{-1} U \quad (3.4)$$

The relative magnitude of  $c_*$  and  $\sigma_1$  is then given by Equations (3.1), (3.3) and (3.4) as

$$\frac{c_*(T_h)}{\sigma_1(T_h)} \geq \begin{cases} 30\alpha_2 \left[ \frac{D_{11}^{\frac{1}{2}}(T_h)}{U} \right] & \text{for } \sigma_1 < O(UL) \\ 5\alpha_2 \left[ \frac{D_{11}^{\frac{1}{2}}(T_h)}{U} \right] \sqrt{\frac{T_h}{L}} & \text{for } \sigma_1 \gg UL, \end{cases} \quad (3.5)$$

Since the minimum prediction time (the argument in the structure function) is normally larger than the integral scale for the small scale turbulence,  $D_{11}(T_h) > 2\sigma_u^2$  (Eidsvik, 12, 13). This means that  $c_*(T_h) > \sigma_1(T_h)$  so that not even the "best" prediction

method for actual wind can predict the location of an initially small passive scalar cloud as accurate as its dimension.

With known  $\tilde{T}_h$  the predicted maximum hazard distance is, as obtained from Equations (2.32) and (3.3):

$$\begin{aligned} \tilde{\theta}_1 &\geq \hat{u}_1 \hat{T}_h + \alpha_2 \tilde{D}_{11}^{\frac{1}{2}}(y) \tilde{T}_h + \tilde{\sigma}_1(T_h) \\ &\geq [\hat{u}_1 + \alpha_2 \tilde{D}_{11}^{\frac{1}{2}}(y)] \tilde{T}_h \end{aligned} \quad (3.7)$$

As for the predicted maximum hazard time, an accurate prediction method for actual weather parameters may therefore reduce the predicted maximum hazard distance by a factor as large as approximately 2.

### 3.3 Transverse dimension

Equation (2.30), (3.1) and (3.4) give:

$$\tilde{\theta}_2(t) \geq \{6 \cdot 10^{-2} + \alpha_1 \left[ \frac{\tilde{D}_{11}^{\frac{1}{2}}(y)}{\bar{U}} \right]\} \tilde{U} t, \quad \text{for } t \ll \tilde{T}_h \quad (3.7)$$

Even with "minimal" prediction error for actual wind estimated by Equation (3.3), the last term dominates. The smaller the  $\tilde{P}_h$ , the more important is a small prediction error for actual wind (direction).

Again it seems likely that the prediction error for actual atmospheric flow, and in particular for actual  $E_c(t)$  will increase the transverse dimension of the hazard area by a factor of approximately 2 so that an accurate prediction method for actual wind might reduce the transverse size of the predicted hazard area by this factor.

4 CONCLUDING REMARKS

Traditionally the accurate prediction of mean cloud size, when the flow parameters are given has attracted most attention. This is not sufficient for the prediction of small hazard areas. With a given prediction error for actual flow parameters, it could even be that an accurate dispersion model gives a larger predicted hazard area than a less accurate one.

Concentration fluctuations may affect the size of the predicted hazard area significantly, but has only received little attention.

The prediction errors for the actual transport velocity (direction), given the flow parameters and prediction errors for the actual flow parameters, has been estimated to affect the size of the predicted hazard area much. Accurate flow prediction could reduce the dimension of the predicted hazard area by a factor as large as 2. However, not even the "best" prediction methods for actual wind can predict an initially small passive scalar clouds location as accurately as its size. This could imply that the simplest diffusion models are accurate enough for this purpose. These aspects of hazard area prediction have apparently not been discussed explicitly before.

The flow prediction aspect is attractive in that it allows control possibilities. By choosing the meteorological prediction (estimation) method in a rational way, the predicted hazard area can be made "cost-effectively" small.

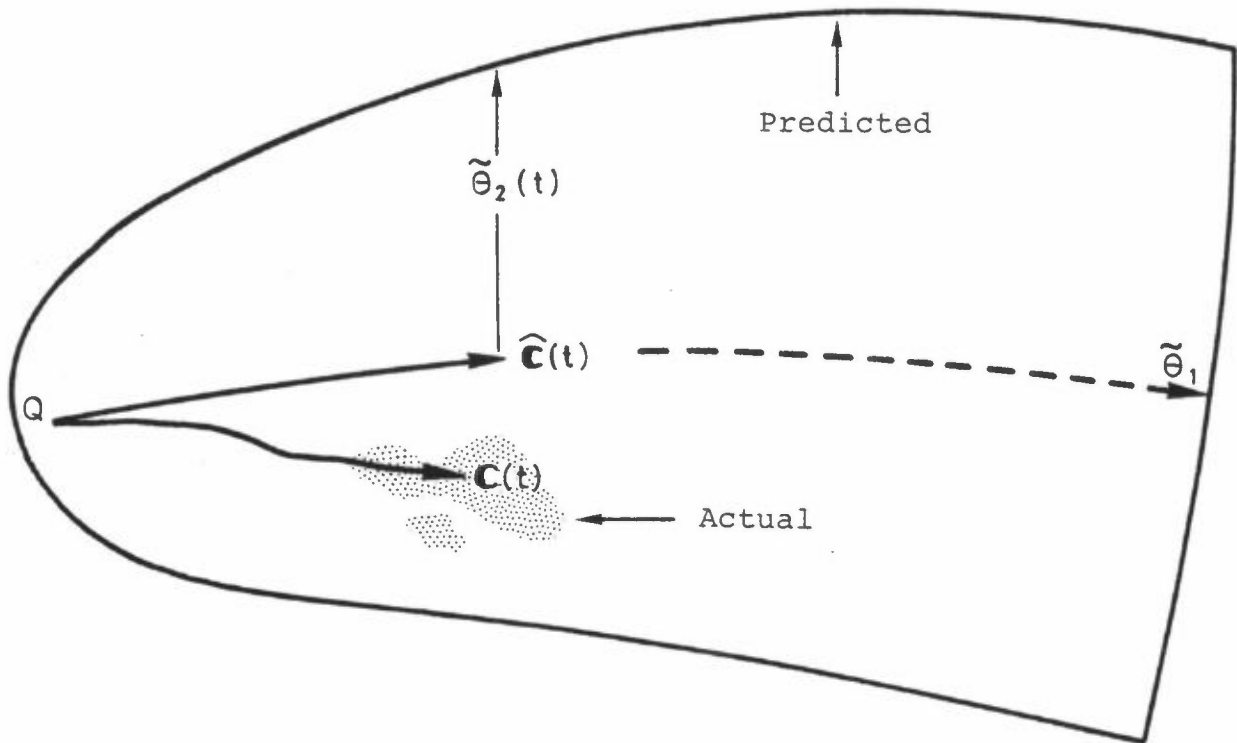


Figure 1: Actual and predicted hazard areas. The predicted area is characterized by the predicted transport vector  $\hat{C}(t)$ , predicted maximum hazard time  $\tilde{T}_h$ , and predicted longitudinal and transverse distances,  $\tilde{\theta}_1(\tilde{T}_h)$  and  $\tilde{\theta}_2(t)$ .





- (9) Eidsvik, K.J. Effects from stochastic atmospheric fields on artillery fire accuracy. Intern Rapport VM-31. Kjeller, Norwegian Defence Research Establishment, 1975.
- (10) Busch, N.E.  
Tennekes, H.  
Panofsky, H.A. Turbulence structure in the planetary boundary layer. *Bound. Layer Meteorol.* 4 211-264 1973.
- (11) Eidsvik, K.J.  
Panofsky, H.A. Turbulence measurements over inhomogeneous terrain. Intern rapport K-236. Kjeller, Norwegian Defence Research Establishment, 1970.
- (12) Eidsvik, K.J. Ekman layer fluctuations modelled as autoregressive integrated moving average stochastic processes. Intern rapport VM-54. Kjeller, Norwegian Defence Research Establishment, 1977.
- (13) Eidsvik, K.J. Identification of models for some time series of atmospheric origin with Akaike's Information Criterion. Lillestrøm, Norwegian Institute for Air Research, 1978. (NILU TN 8/79.)